Vol 18 No 7, July 2009
1674-1056/2009/18(07)/2719-05

Chinese Physics B

© 2009 Chin. Phys. Soc.
and IOP Publishing Ltd

Dynamical entanglement for Fermi coupled stretching and bending modes*

Hou Xi-Wen(侯喜文)[a] and Cheng Chuan-Ming(成传明)[b]

[a] *Department of Physics, Huazhong Normal University, Wuhan* 430079, *China*
[b] *Department of Physics and Electronic Engineering, Yunyang Teachers' College, Danjiangkou* 442700, *China*

(Received 6 July 2008; revised manuscript received 6 November 2008)

The dynamical entanglement for Fermi coupled C–H stretch and bend vibrations in molecule CHD_3 is studied in terms of two negativities and the reduced von Neumann entropy, where initial states are taken to be direct products of photon-added coherent states on each mode. It is demonstrated that the negativity defined by the sum of negative eigenvalues of the partial transpose of density matrices is positively correlated with the von Neumann entropy. The entanglement difference between photon-added coherent states and usual coherent states is discussed as well.

Keywords: vibrational analysis, quantum entanglement
PACC: 3310G, 0365

1. Introduction

Entanglement has recently generated a lot of activity among researchers, owing to its significant role in the realization of quantum computation and quantum information. This leads to the study of entanglement characteristics in various systems.[1−8] For Bose–Einstein condensates (BEC), the maximum entanglement between the atomic and molecular modes in an atom-molecule BEC occurs for different parameter values.[3] In addition, entanglement approaching maximal value can be achieved with nonlinear interactions[4] or at the point of dynamical phase transition in the BEC in a symmetric double well.[5] Similarly, the nonlinear interaction between excitons in two coupled semiconductor microcrystallites increases the values of entanglement more than that of the linear coupling model.[7] For two stretching vibrations in triatomic molecules, it is shown that the entanglement of initial Fock states with local-mode character is regular while that of states with normal-mode character is irregular.[8] References [3]–[8] consider the specific Hamiltonian which is symmetric in the two modes with identical nonlinear terms and a symmetric coupling between the modes, where entanglement of Fock states[3,4,7,8] and coherent states[6] is measured in terms of the reduced linear entropy and von Neumann entropy. However, this symmetry is not expected to be presented in a generic Hamiltonian governing the interaction in other systems, for instance, in molecules such as CHD_3, where Fermi resonances between the stretching and bending vibrational states must be taken into account. More importantly, Fermi resonances play a key role in the mechanism of intramolecular vibrational energy redistribution.[9] In the present work, we shall investigate the properties of entanglement for the C–H bend and stretch modes in a model based on experimental spectra of molecule CHD_3.

There are various measures of entanglement in the literature. Although a particular measure of entanglement can be analytically determined in some cases, most entanglement measures are very difficult to calculate in general.[10] The calculation of a more tractable measure can allow one to work out the correct ordering of density matrices for other measures.[10,11] Various measures for maximally entangled mixed states have been characterized in Ref.[12]. It is shown that the maximally entangled mixed states depend on the measures which one uses to quantify entanglement and the measures of mixedness.[12] However, Refs.[10]–[12] are restricted to static properties of entanglement. As those quantities of entanglement which are useful in characterizing entangled states are defined in a quite different manner, they must lead to dynamical difference for a state. The degree of dynamical difference among those measures for a common initial state is critically important in the more effective realization of the quantum information process and some tasks. To examine that difference can at least help one to construct a standard measure of entanglement among so many quantities. It is now understood that the linear entropy and von Neumann entropy have the same trend for a bipar-

*Project supported by the National Natural Science Foundation of China (Grant No 10675050).

tite system.[12,13] We shall use two negativities[12,14] and von Neumann entropy to measure entanglement for their simplicity as well as their wide applicability, in order to perform a dynamical comparison of those three measures in CHD_3. The dynamics of entanglement is studied for specific non-entangled initial states of interest: namely, those in which each mode is initially in a photon-added coherent state (PACS).[15]

The PACS is originally introduced as an initial state of a single-mode radiation field in the description of interactions between the field and atoms.[15] The PACS has some interesting properties such as a quantifiable degree of departure from perfect coherence, sub-Poisson statistics, and phase-squeezing.[15] In addition, PACS is a kind of continuous-variable-type state, which in a special case reduces to the usual coherent state (CS). Furthermore, a single-added coherent state has recently been generated experimentally and characterized by using quantum tomography.[16] Here PACSs are used to inspect the time-evolution of entanglement in CHD_3. The importance of studying in detail those in different initial states is twofold. It may be viewed as a key to the understanding of some of the striking differences between the quantum and classical description of the world. Continuous-variable-type entangled states including coherent states have been widely applied to quantum teleportation,[17] quantum cryptography,[18] and quantum computation.[19] Therefore it is an interesting topic to study the dynamical entanglement of PACSs. Section 2 presents the Hamiltonian for experimental CH-stretching and bending spectra in CHD_3. Section 3 is devoted to studying the dynamical entanglement of PACSs. A conclusion and discussion are given in last section.

2. Effective Hamiltonian

An effective Hamiltonian for experimental CH-stretching and bending spectra in CHD_3 reads[20]

$$\begin{aligned} H =& \omega_{\rm s}\left(a_{\rm s}^{\dagger}a_{\rm s}+\frac{1}{2}\right)+\omega_{\rm b}(a_{\rm b}^{\dagger}a_{\rm b}+1) \\ &+X_{\rm ss}\left(a_{\rm s}^{\dagger}a_{\rm s}+\frac{1}{2}\right)^2+X_{\rm bb}(a_{\rm b}^{\dagger}a_{\rm b}+1)^2 \\ &+X_{\rm sb}\left(a_{\rm s}^{\dagger}a_{\rm s}+\frac{1}{2}\right)(a_{\rm b}^{\dagger}a_{\rm b}+1) \\ &+K_{\rm sbb}\left(a_{\rm s}^{\dagger}a_{\rm b}a_{\rm b}+a_{\rm s}a_{\rm b}^{\dagger}a_{\rm b}^{\dagger}\right), \end{aligned} \tag{1}$$

where a_i and $a_i^{\dagger}$ ($i=$ s, b) are the annihilation and creation operators on the C–H stretch and bend modes, respectively, and $\omega_{\rm s}$, $\omega_{\rm b}$, $X_{\rm ss}$, $X_{\rm bb}$, $X_{\rm sb}$, and $K_{\rm sbb}$ have their usual spectroscopic meaning with $K_{\rm sbb}$ being the Fermi coupling parameter between the stretch and the bend. The quantum Hamiltonian (1) conserves a quantum number, called the polyad quantum number, $N=v_{\rm s}+\frac{1}{2}v_{\rm b}$. The quantum density of states for the Hamiltonian (1) was analyzed in terms of semiclassical periodic orbit theory,[21] where the vibrational angular momentum (l) was taken to be 0. We shall also work in the $l=0$ subspace throughout, and so label basis states with two quantum numbers only: $|v_{\rm s},v_{\rm b}\rangle$. Diagonalization of the Hamiltonian (1) in the basis states gives the quantum spectrum with the corresponding eigenvectors. Fitting highly excited spectra of CHD_3, Lewerenz and Quack have presented the optimized parameters in Table VII in Ref.[20], which are reproduced in $\rm cm^{-1}$ as follows: $\omega_{\rm s}=3047.04$, $\omega_{\rm b}=1293.35$, $X_{\rm ss}=-57.91$, $X_{\rm bb}=-4.49$, $X_{\rm sb}=-22.12$, and $K_{\rm sbb}=-25.84$. From those parameters, anharmonic interactions ($X_{\rm ss}$, $X_{\rm bb}$, $X_{\rm sb}$, and $K_{\rm sbb}$) are of importance for the experimental band centres of CHD_3.

3. Entanglement dynamics

We now investigate the entanglement dynamics of an initial state which is a direct product of PACSs on each mode. Entanglement of two modes sets in during temporal evolution. The initial state of the full system is taken to be

$$|\psi(0)\rangle = |\psi_{\rm s}(0)\rangle\otimes|\psi_{\rm b}(0)\rangle, \tag{2}$$

where $|\psi_i(0)\rangle$ is taken to be a PACS, given by Ref.[15]

$$|\psi_i(0)\rangle = \frac{(a_i^{\dagger})^m|\alpha\rangle_i}{\sqrt{{}_i\langle\alpha|a_i^m a_i^{\dagger m}|\alpha\rangle_i}} = \frac{(a_i^{\dagger})^m|\alpha\rangle_i}{\sqrt{m!L_m(-\nu)}}, \tag{3}$$

where $|\alpha\rangle_i=\mathrm{e}^{-\frac{|\alpha|^2}{2}}\sum_{v_i=0}^{\infty}\frac{\alpha^{v_i}}{\sqrt{v_i!}}|v_i\rangle$ is the usual CS on mode i ($i=$ s, b) with $|v_i\rangle$ being a Fock state, $\alpha\in\mathcal{C}$, $\nu=|\alpha|^2$, and L_m is the Laguerre polynomial of order m (positive integer). It is easy to see that Eq.(3) with $m=0$ reduces to CS with the Poisson distribution. Note that Eq.(3) with $m\neq 0$ has the sub-Poisson distribution. Here we consider the cases of $m=0$, 1, and 3 with ν on each mode being taken to be the same value. For other values of m and ν it is straightforward to simulate the entanglement dynamics.

We are interested in negativity as a measure of entanglement since it can be computed efficiently for any states of an arbitrary bipartite system. The negativity of a state $\rho_{\rm bc}(t)$ is defined by Ref.[12],

$$N_{\rm s}(t)=\max\{0,-\lambda_{\rm neg}\}, \tag{4}$$

where $\lambda_{\rm neg}$ is the sum of the negative eigenvalues of $\rho^{\rm T_2}_{i\alpha,j\beta}(t)$, which is given by

$$\rho^{\rm T_2}_{i\alpha,j\beta}(t) \equiv \rho_{i\beta,j\alpha}(t), \tag{5}$$

where $\rm T_2$ is partial transposition for the second subsystem.

The negativity is also simply defined by Ref.[14],

$$N(t) = \max\{0, -\mu_{\rm min}\}, \tag{6}$$

where $\mu_{\rm min}$ is the minimum of the eigenvalues of the partial transpose of state $\rho_{\rm bc}(t)$.

As we are dealing with a pure bipartite system, the entanglement can be described by the reduced von Neumann entropy $s(t)$, defined by Ref.[22],

$$s(t) = -{\rm Tr_b}\boldsymbol{\rho}_{\rm b}(t)\ln\boldsymbol{\rho}_{\rm b}(t), \tag{7}$$

where $\rm Tr_b$ denotes a trace over the bending mode, and $\boldsymbol{\rho}_{\rm b}(t)$ is the reduced-density matrices, $\boldsymbol{\rho}_{\rm b}(t) = {\rm Tr_s}|\psi(t)\rangle\langle\psi(t)|$, where indexes b and s stand for the degree of freedom on the bend and the stretch, respectively, and $|\psi(t)\rangle$ is the quantum state of the full system which evolves in time under the action of the Hamiltonian (1). The entropy can be described in terms of the reduced linear entropy, $1 - {\rm Tr_b}[\boldsymbol{\rho}_{\rm b}(t)]^2$. Both entropies have the same trend for a bipartite system[13] so that the results of von Neumann entropy are presented in the following.

Figure 1 shows the entanglement dynamics measured by two negativities, $N_{\rm s}(t)$ (solid line) and $N(t)$ (dash-dotted line), and von Neumann entropy $s(t)$ (dashed line) for PACSs with $m = 0$ for (a) and (b), $m = 1$ for (c) and (d), and $m = 3$ for (e) and (f), $\nu = 0.2$ in Figs.1(a), 1(c), and 1(e), and $\nu = 1.5$ in Figs.1(b), 1(d), and 1(f), for example. A number of observations in Fig.1 are as follows.

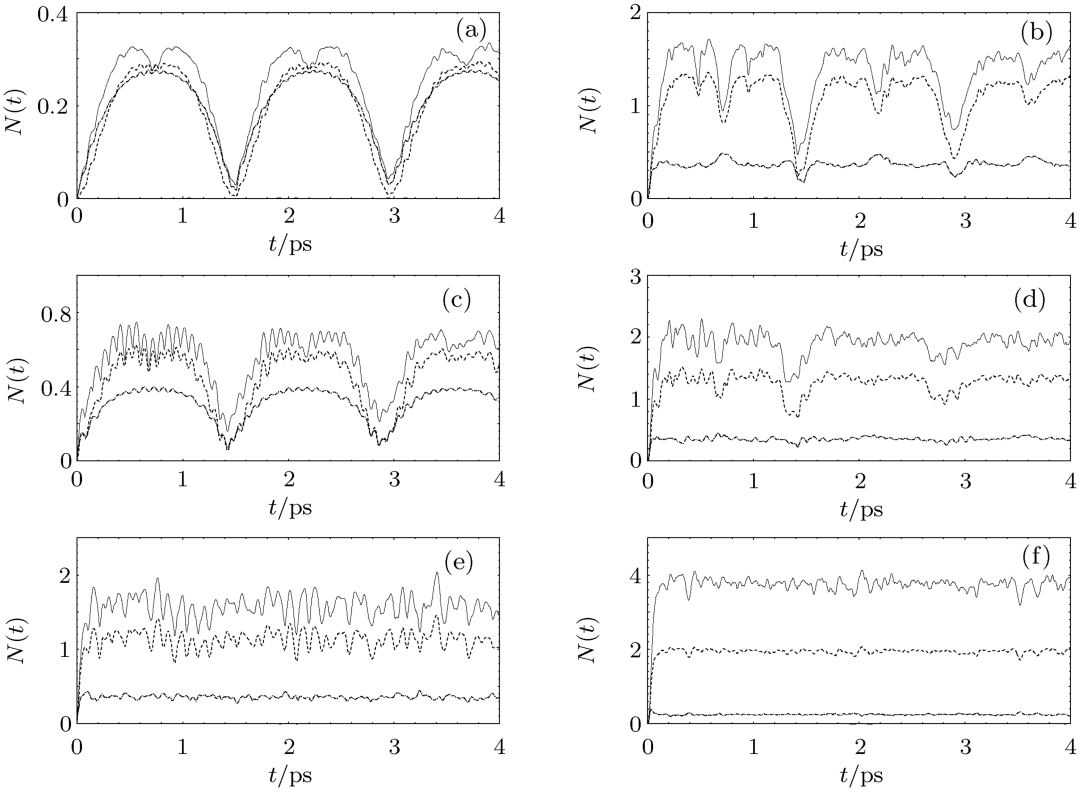


Fig.1. Two negativities, $N_{\rm s}(t)$ (solid line) and $N(t)$ (dash-dotted line), and von Neumann entropy $s(t)$ (dashed line) for PACSs with $m = 0$ for (a) and (b), $m = 1$ for (c) and (d), and $m = 3$ for (e) and (f), $\nu = 0.2$ for (a), (c), and (e), and $\nu = 1.5$ for (b), (d), and (f). Note that the scale of the horizontal axis is the same while that of the vertical axis is different.

Firstly, we compare both negativities with von Neumann entropy since they are good measures of entanglement for a pure separable state as well as being dimensionless. Two qualitative different correlations of those three measures are discovered in Fig.1. The first type of correlation is a case where two measures rise and lower

together, and the second type of correlation is a case where they are anti-correlated, that is, one measure increases with time while another decreases or vice versa. For the same initial state, it is evident that negativity $N_{\rm s}(t)$ is positively correlated with von Neumann entropy $s(t)$, where the value of $N_{\rm s}(t)$ is the largest among three measures in any instant of time while that of $N(t)$ is the smallest. For the PACS with $m = 0, 1$ and with a small parameter $\nu = 0.2$ in Figs.1(a) and 1(c), negativity $N(t)$ is dominant in positive correlation with von Neumann entropy $s(t)$ and negativity $N_{\rm s}(t)$, whereas it is positively correlated or anti-correlated with latter in an irregular manner in Figs.1(b), 1(d), 1(e) and 1(f).

Secondly, for small parameter $\nu = 0.2$, three measures for CS ($m = 0$) display nice periodicity with a rapid oscillation in a small amplitude, as shown in Figs.1(a), 1(c) and 1(e). Such a periodicity partly remains for PACS with $m = 1$ with a similar oscillation while that with $m = 3$ breaks down with a rapid pulsed oscillation in a large amplitude. Thus, for a small value of ν, it is easy to distinguish between an initial CS and an initial PACS in entanglement pulsed oscillation with a large amplitude. For a large parameter $\nu = 1.5$, three measures for CS and PACS are irregular, as shown in Figs.1(b), 1(d) and 1(f). However, the oscillatory amplitude for $m = 3$ is the smallest. It should be mentioned that the small-amplitude oscillations of von Neumann entropy may be regarded as fingerprints of the underlying classical chaos in smooth Hamiltonian systems.[23] Thus such behaviour in Fig.1(f) is due to a specific initial state and the anharmonic interactions in Hamiltonian (1). Comparing Fig.1(a) with 1(b), 1(c) with 1(d), and 1(e) with 1(f), one can find that for a given m, the maximal entanglement and the increasing rate of entanglement in the early-time evolution increase with increasing ν, where the oscillatory frequency of entanglement becomes faster. It comes from the fact that more states take part in the entanglement evolution.

It is possible to explain the above mentioned period for the PACS with small parameter $\nu = 0.2$ in Fig.1(a). The initial PACS with $m = 0$ can be approximatively taken to be

$$\begin{aligned} &|\psi(0)\rangle \\ \cong\ & P(0,0)|0,0\rangle + P(0,1)|0,1\rangle + P(1,0)|1,0\rangle \\ &+P(0,2)|0,2\rangle + P(1,1)|1,1\rangle + P(0,3)|0,3\rangle, \end{aligned} \tag{8}$$

where $P(v_{\rm s}, v_{\rm b}) = {\rm e}^{-|\alpha|^2} \dfrac{\alpha^{v_{\rm s}+v_{\rm b}}}{\sqrt{v_{\rm s}! v_{\rm b}!}}$, $|v_{\rm s}, v_{\rm b}\rangle = |v_{\rm s}\rangle \otimes |v_{\rm b}\rangle$, $v_{\rm s(b)}$ is the vibrational quantum number on bond s (b). That state evolves as follows:

$$\begin{aligned} |\psi(t)\rangle \ =\ & P(0,0){\rm e}^{-{\rm i}H_0(0,0)t}|0,0\rangle + {\rm e}^{-{\rm i}H_0(0,1)t}|0,1\rangle \\ &+{\rm e}^{-{\rm i}\sigma_1 t}\left\{\left[P(1,0)\cos(\omega_1 t) - {\rm i}\frac{P(1,0)\sigma_2 + 2P(0,2)K_{\rm sbb}}{\omega_1}\sin(\omega_1 t)\right]|1,0\rangle\right. \\ &\left.+\left[P(0,2)\cos(\omega_1 t) - {\rm i}\frac{2P(1,0)K_{\rm sbb} - P(0,2)\sigma_2}{\omega_1}\sin(\omega_1 t)\right]|0,2\rangle\right\} \\ &+{\rm e}^{-{\rm i}\sigma_3 t}\left\{\left[P(1,1)\cos(\omega_2 t) - {\rm i}\frac{P(1,1)\sigma_4 + 3P(0,3)K_{\rm sbb}}{\omega_2}\sin(\omega_2 t)\right]|1,1\rangle\right. \\ &\left.+\left[P(0,3)\cos(\omega_2 t) - {\rm i}\frac{3P(1,1)K_{\rm sbb} - P(0,3)\sigma_4}{\omega_2}\sin(\omega_2 t)\right]|0,3\rangle\right\}, \end{aligned} \tag{9}$$

where $H_0(v_{\rm s}, v_{\rm b}) = \omega_{\rm s}\left(v_{\rm s} + \dfrac{1}{2}\right) + \omega_{\rm b}(v_{\rm b} + 1) + X_{\rm ss}\left(v_{\rm s} + \dfrac{1}{2}\right)^2 + X_{\rm bb}(v_{\rm b} + 1)^2 + X_{\rm sb}\left(v_{\rm s} + \dfrac{1}{2}\right)(v_{\rm b} + 1)$, $\sigma_1 = [H_0(1,0) + H_0(0,2)]/2$, $\sigma_2 = [H_0(1,0) - H_0(0,2)]/2$, $\omega_1 = \sqrt{4K_{\rm sbb}^2 + \sigma_2^2}$, $\sigma_3 = [H_0(1,1) + H_0(0,3)]/2$, $\sigma_4 = [H_0(1,1) - H_0(0,3)]/2$, and $\omega_2 = \sqrt{9K_{\rm sbb}^2 + \sigma_4^2}$. Therefore, two negativities, $N_{\rm s}(t)$ and $N(t)$, and von Neumann entropy $s(t)$ can be expressed in an analytic form which is too lengthy to include here. For $\nu = 0.2$ the longest period of three measures by Eq.(9) is given by

$$T = \frac{2\pi}{\omega_{\rm m}}, \tag{10}$$

where $\omega_{\rm m} = H_0(0,1) + \sigma_1 - \sigma_3 + \omega_1 - \omega_2$, is the minimal frequency of entanglement since other frequencies are much larger than $\omega_{\rm m}$. Thus the value of period by Eq.(10) is 1.578 ps, which is quite close to the corresponding periods 1.50 ps obtained in Fig.1(a). With Eq.(9), the maximal entropy of $s(t)$ is indeed larger than that of $N(t)$, while $N_{\rm s}(t)$ and $N(t)$ have nearly

the same value. However, there is a large difference in the amplitude of three measures between analytical and numerical calculation. This is because the analytical calculation is performed with a simplified model. For other states in Fig.1, it is probably impossible to get an analytic expression of those measures since more Fock states with higher quantum number run into the entanglement evolution.

Thirdly, for a given parameter ν, the maximal entanglement and the increasing rate of entanglement in the early-time evolution increase as m increases, where the evolution of entanglement becomes more irregular. This is because the highly excited states higher than m in PACS on each mode have a significant contribution to entanglement evolution. Thus, PACS with a larger m can be used to get a maximal entanglement.

Finally, it is noted that the entanglement of CS and PACS with $m = 1$ has larger excursions back to near zero with larger values of ν. The time of the first excursion of CS is longer than that of PACS with $m = 1$. For PACS with $m = 3$, those excursions are replaced by rapid pulsed oscillations since highly excited states have a large contribution to entanglement. In the simulation of entanglement dynamics it is found that those excursions are farther from zero in long time evolution.

4. Conclusion and discussion

In summary, we have investigated dynamical entanglement of direct products of PACS on C–H stretch and bend vibrations in molecule CHD_3, where the entanglement is measured by two negativities and von Neumann entropy. It is shown that negativity $N_{\rm s}(t)$ is positively correlated with von Neumann entropy $s(t)$ with the value of $N_{\rm s}(t)$ being the largest among those three measures in any instant of time. For the PACS with $m = 0, 1$ with a small parameter, negativity $N(t)$ is dominant in positive correlation with von Neumann entropy $s(t)$ and negativity $N_{\rm s}(t)$. It is demonstrated that for a given parameter ν, a maximum entanglement for PACS with a large m can be obtained, and the oscillatory frequency for PACS is smaller than that for CS. It provides a simple manner to distinguish between an initial CS and an initial PACS in dynamical entanglement. We believe that these can be useful in molecular quantum computing since the computing based on vibrational states of diatomic molecules[24] is feasible.

It is desirable to use those properties for molecular quantum computing. It is worthwhile to explore the behavior of entanglement in other molecules.[25]

References

[1] Cheng R and Liang J Q 2007 *Chin. Phys.* **16** 834
Xi X Q and Liu W M 2007 *Chin. Phys.* **16** 1858
Yang X, Xiang S H and Song K H 2008 *Chin. Phys.* B **17** 435

[2] Gong L Y and Tong P Q 2008 *Chin. Phys.* B **17** 674
Fang M F, Feng Y Z, Hu Y H and Wu Q 2008 *Chin. Phys.* B **17** 2963
Zhang Y J, Zhou Y and Xia Y J 2008 *Acta Phys. Sin.* **57** 21 (in Chinese)
Ma X S and Wang A M 2008 *Acta Phys. Sin.* **57** 2026 (in Chinese)

[3] Hines A P, McKenzie R H and Milburn G J 2003 *Phys. Rev.* A **67** 013609

[4] Choi S and Bigelow N P 2005 *Phys. Rev.* A **72** 033612

[5] Fu L and Liu J 2006 *Phys. Rev.* A **74** 063614

[6] Sanz L, Angelo R M and Furuya K 2003 *J. Phys.* A **36** 9737

[7] Liu Y X, Özdemir S K, Miranowicz A, Koashi M and Imoto N 2004 *J. Phys.* A **37** 4423

[8] Hou X W, Chen J H and Ma Z Q 2006 *Phys. Rev.* A **74** 062513
Liu D M, Peng D P and Hou X W 2008 *Chin. Phys. Lett.* **25** 1263

[9] Talanina I B and Collins M A 1993 *J. Chem. Phys.* **98** 1817

[10] Virmani S and Plenio M B 2000 *Phys. Lett.* A **268** 31

[11] Ziman M and Buzek V 2006 *Phys. Rev.* A **73** 012312
Kinoshita Y, Namiki R, Yamamoto T, Koashi M and Imoto N 2007 *Phys. Rev.* A **75** 032307

[12] Wei T C, Nemoto K, Goldbart P M, Kwiat P G, Munro W J and Verstraete F 2003 *Phys. Rev.* A **67** 022110

[13] Boukobza E and Tannor D J 2005 *Phys. Rev.* A **71** 063821

[14] Peres A 1996 *Phys. Rev. Lett.* **77** 1413

[15] Agarwal G S and Tara K 1991 *Phys. Rev.* A **43** 492

[16] Zavatta A, Viciani S and Bellini M 2005 *Science* **306** 660

[17] Cochrane P T, Milburn G T and Munro W J 2000 *Phys. Rev.* A **62** 062307

[18] Gottesman D and Preskill J 2001 *Phys. Rev.* A **63** 022309

[19] Munro W J, Milburn G J and Sanders B C 2000 *Phys. Rev.* A **62** 052108

[20] Lewerenz M and Quack M 1988 *J. Chem. Phys.* **88** 5408

[21] Ezra G S 1996 *J. Chem. Phys.* **104** 26

[22] Lichtner P C and Griffin J J 1976 *Phys. Rev. Lett.* **37** 1521
Zurek W H, Habib S and Paz J P 1993 *Phys. Rev. Lett.* **70** 1187

[23] Gong J and Brumer P 2003 *Phys. Rev.* A **68** 022101

[24] Cheng T and Brown A 2006 *J. Chem. Phys.* **124** 034111

[25] Hou X W, Wan M F and Ma Z Q 2008 *Opt. Commun.* **281** 3587